Mangal et al., https://doi.org/10.1083/jcb.201706021

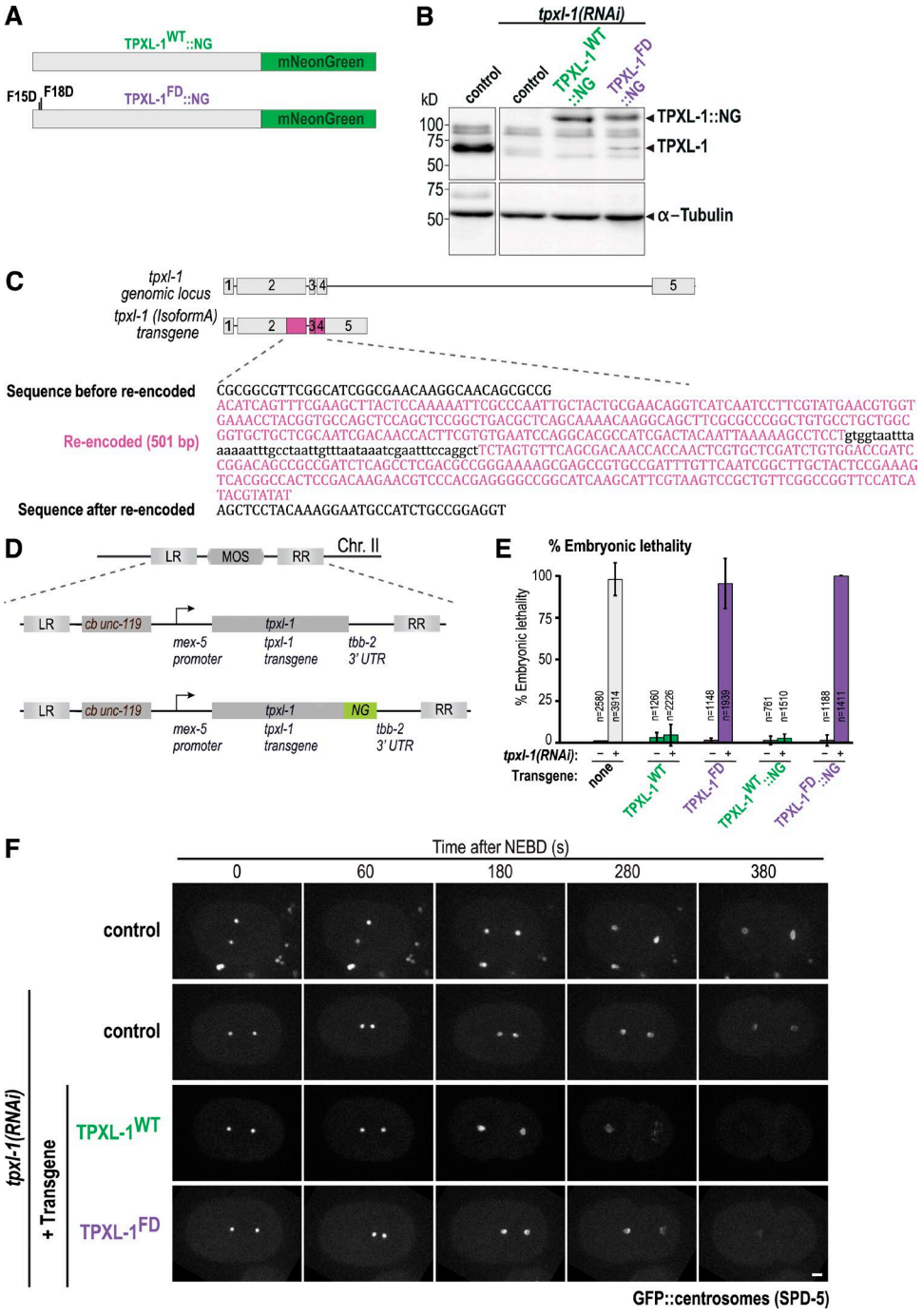

Figure S1. **Transgenes encoding WT untagged and mNeonGreen tagged TPXL-1 are functional.** Related to Figs. 4 and 5. **(A)** Schematics showing TPXL-1^{WT} or TPXL-1^{FD} tagged with mNeonGreen. **(B)** Immunoblots of control (N2) and transgenic animals expressing RNAi-resistant TPXL-1^{WT}::NG or TPXL-1^{FD}::NG after depletion of endogenous TPXL-1 by RNAi. Immunoblots were probed for TPXL-1 and α-tubulin as a loading control. **(C)** Schematic representation of intron-exon organization of the *C. elegans tpxl-1* gene. To make the *tpxl-1* transgene RNAi resistant, a region including exon 3 and parts of exons 2 and 4 was reencoded. The intron between exons 2 and 3 was maintained, but the long intron between exons 4 and 5 was deleted. **(D)** The untagged and NG-tagged TPXL-1 transgenes, under control of the *mex-5* promoter and *tbb-2* 3′ UTR, were integrated into chromosome II using MosSCI (Frøkjaer-Jensen et al., 2008). **(E)** Graph plotting percentage embryonic lethality for the indicated conditions. Error bars are SD; *n* = number of progeny analyzed. **(F)** Maximum-intensity projections of five confocal planes (1.5 µm apart) of embryos expressing GFP::SPD-5 with TPXL-1^{WT} or TPXL-1^{FD} or without a transgene (control). Endogenous TPXL-1 was depleted by RNAi. The distance between the two centrosomes was measured and is quantified in Fig. 5 C. Time after NEBD is indicated. Bar, 5 µm.

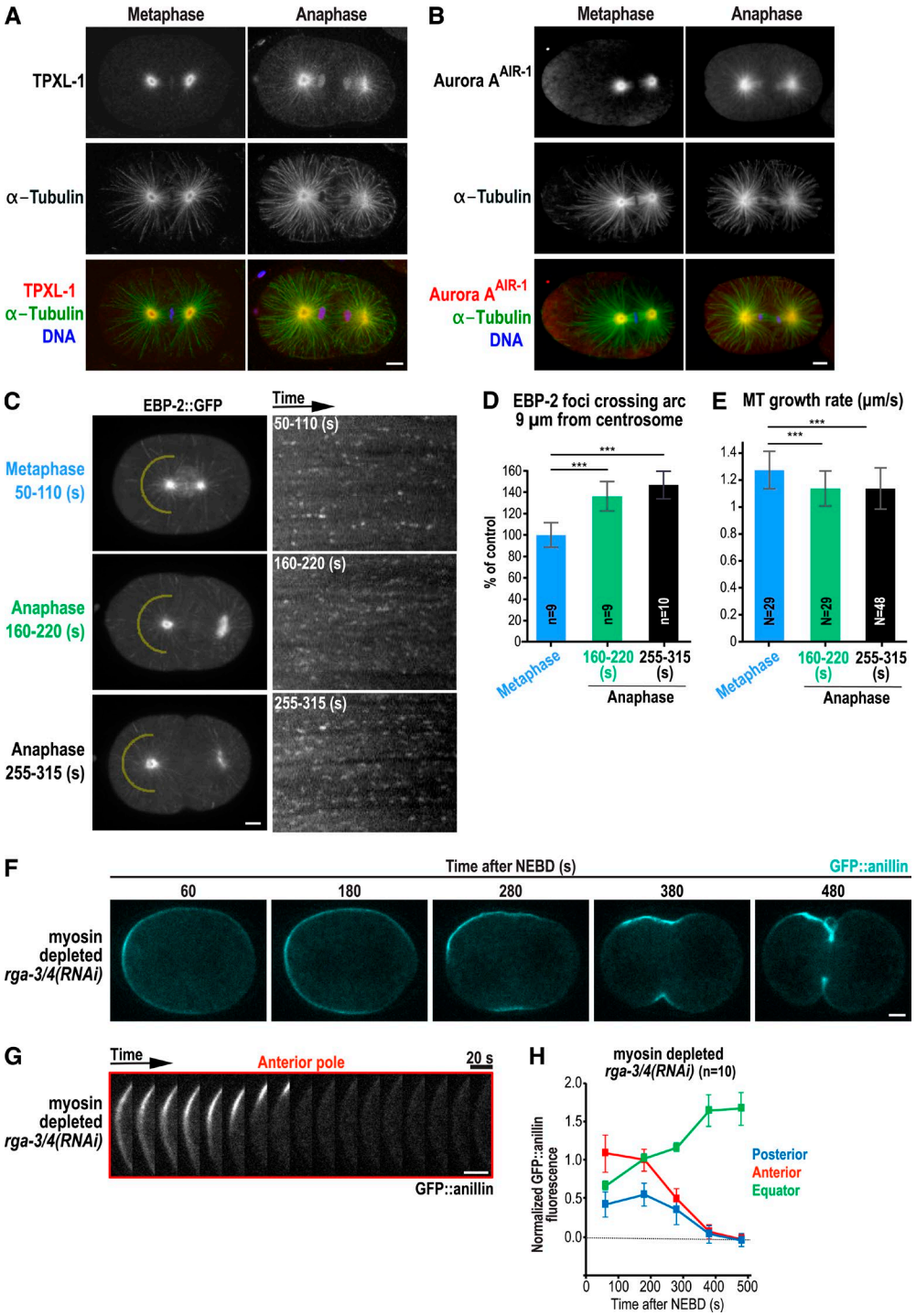

Figure S2. **Endogenous TPXL-1 and Aurora A^{AIR-1} localize to astral microtubules in anaphase.** Related to Fig. 4. **(A)** Confocal images of fixed metaphase and anaphase embryos stained for endogenous TPXL-1, α-tubulin, and DNA (prometaphase and metaphase, *n* = 8; anaphase, *n* = 9 embryos). To visualize astral microtubules without saturating the aster centers, a gamma of 2 was introduced in Photoshop for all images, which were scaled identically. **(B)** Confocal images of fixed metaphase (*n* = 5) and anaphase (*n* = 5) embryos stained for Aurora A^{AIR-1}, α-tubulin, and DNA. To visualize astral microtubules without saturating the aster centers, a gamma of 1.5 was applied to all images in Photoshop, which were scaled identically. **(C)** Representative projections of the images acquired every 400 ms over a 4-s interval in metaphase (*n* = 9), early anaphase (160–220 s after NEBD; *n* = 9), and late anaphase (255–315 s after NEBD; *n* = 10) control embryos expressing EBP-2::GFP. To visualize EBP-2::GFP without saturating the aster centers, a gamma of 1.2 was introduced in Photoshop. Kymographs generated for the indicated conditions (right) were used to count the number of EBP-2::GFP foci that crossed an arc 9 µm away from the anterior centrosome (yellow). **(D and E)** Graphs plot the number of EBP-2::GFP foci crossing an arc 9 µm from the centrosome (D) and the microtubule growth rates (E) at the indicated times in control embryos. Error bars are SD; p-values are two-tailed Student's *t* test (***, P < 0.001); *n* = number of embryos in D; *N* = number of microtubules tracked in three or more embryos per condition in E. **(F)** Representative time-lapse images of the first division of a myosin-depleted *rga-3/4(RNAi)* embryo expressing GFP::anillin (cyan, *n* = 5 embryos). Time points are seconds after NEBD. **(G)** Kymograph of the anterior pole of the embryo in F beginning 180 s after NEBD. **(H)** Normalized cortical GFP::anillin fluorescence was quantified as depicted in Fig. 1 F and is plotted for the anterior (red), posterior (blue) and equatorial (green) cortex in myosin-depleted *rga-3/4(RNAi)* embryos. Error bars are SEM and *n* = number of linescans. Bars, 5 µm.

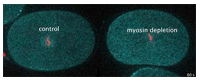

Video 1. ***C. elegans* one-cell embryos expressing GFP::anillin (cyan) and mCherry::histone (red) without (control, left) and with (right) myosin depletion.** Related to Fig. 1. Images were acquired every 20 s on an UltraVIEW VoX spinning disk confocal microscope (PerkinElmer) attached to an Axio Observer D1 stand (Zeiss), equipped with a 63× 1.4-NA Plan-Apochromat oil immersion objective and a EMCCD C9100-50 camera (1,000 × 1,000 pixels). Video starts 60 s after NEBD. Playback rate is 60× real time (3 frames/s).

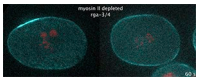

Video 2. **Two representative myosin-depleted *rga-3/4Δ* embryos expressing GFP::anillin (cyan) and mCherry::histone (red).** Related to Fig. 1. Images were acquired as described in Video 1 every 20 s. Video starts 60 s after NEBD. Playback rate is 60× real time (3 frames/second).

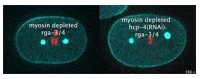

Video 3. **Myosin-depleted *rga-3/4Δ C. elegans* embryos without (left) and with *hcp-4(RNAi)* (right) expressing GFP::anillin and a GFP-tagged centrosome marker (cyan) along with mCherry::histone (red).** Related to Fig. 2. Images were acquired as described in Video 1 every 20 s. Playback rate is 60× real time (3 frames/s). Video starts 180 s after NEBD.

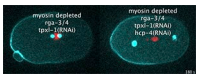

Video 4. **Myosin-depleted *rga-3/4Δ C. elegans* embryos expressing GFP::anillin and a GFP-tagged centrosome marker (cyan) along with mCherry::histone (red).** Related to Fig. 3. TPXL-1 (left) or TPXL-1 and HCP-4 (right) were additionally depleted by RNAi. Images were acquired as described in Video 1 every 20 s. Playback rate is 60× real time (3 frames/s). Video starts 180 s after NEBD.

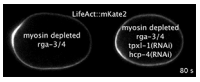

Video 5. **Myosin-depleted *rga-3/4Δ C. elegans* embryos expressing LifeAct::mKate2.** Related to Fig. 3. HCP-4 (left) or HCP-4 and TPXL-1 (right) were additionally depleted by RNAi. Images were acquired every 20 s on a Nikon eclipse Ti spinning disk confocal controlled by NIS Elements 4.51 software equipped with a 100× 1.45-NA Plan-Apochromat oil immersion objective and Andor DU-888 X11056 camera. Elapsed time and anaphase onset are indicated. Playback rate is 60× real time (3 frames/s). Video starts 80 s after NEBD.

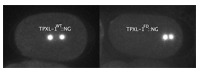

Video 6. **Representative examples of *C. elegans* embryos expressing TPXL-1^{WT}::NG (left) or TPXL-1^{FD}::NG (right) from RNAi-resistant transgenes after depletion of endogenous TPXL-1 by RNAi.** Related to Fig. 4. Images were acquired as described in Video 5. To visualize TPXL-1 localization on astral microtubules without saturating the astral centers, a gamma of 0.5 was introduced in Fiji. Elapsed time and anaphase onset are indicated.

Video 7. ***C. elegans*one-cell control (left), myosin-depleted *rga-3/4(RNAi)* (middle), or myosin-depleted *hcp-4 tpxl-1(RNAi)* (right) embryos expressing EBP-2::GFP.** Related to Fig. 4. Images were acquired as described in Video 5 every 400 ms. Playback rate is 2.4× real time (6 frames/s). To visualize EBP-2::GFP without saturating the aster centers, a gamma of 0.7 was introduced in Fiji. Movie starts 255 s after NEBD.

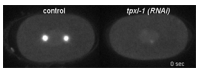

Video 8. **Representative examples of *C. elegans* embryos expressing GFP::Aurora A^{AIR-1} without (left) and with *tpxl-1(RNAi)* (right).** Related to Fig. 4. Images were acquired as described in Video 5. To visualize GFP::Aurora A^{AIR-1} localization on astral microtubules without saturating the aster centers, a gamma of 0.6 was introduced in Fiji. Elapsed time and anaphase onset are indicated.

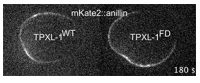

Video 9. **Representative myosin-depleted *rga-3/4Δ C. elegans* embryos expressing TPXL-1^{WT} (left) or TPXL-1^{FD} (right) together with mKate2::anillin.** Related to Fig. 5. Embryos were additionally depleted of endogenous TPXL-1 and HCP-4 by RNAi. Images were acquired as described in Video 1 every 20 s. Playback rate is 60× real time (3 frames/s). Video starts 180 s after NEBD.

Table S1. ***C. elegans* strains**

Strain name	Genotype	Reference
N2	Wild type (ancestral)	
OD184	ltIs108 [pOD564/pFM005; pie-1::LAP::AIR-1^{WT} reencoded; unc-119(+)]	This study
OD296	ltIs37 [pAA64; pie-1/mCherry::his-58; unc-119 (+)] IV; ltIs28 [pASM14; pie-1/GFP-TEV- Stag::ANI-1; unc-119 (+)];	Zanin et al., 2013
OD314	unc-119(ed3) III; ltIs37 [pAA64; pie-1/mCherry::his-58; unc-119 (+)] IV; ltIs28 [pASM14; pie-1/GFP-TEV-Stag::ANI-1; unc-119 (+)]; rga-4(ok1935) unc-62(e644) rga-3(ok1988) V/nT1[qIs51] (IV;V)	Zanin et al., 2013
OD847	unc-119(ed9) III; ltSi202 [pVV103/ pOD1021; Pspd-2::GFP::SPD-5 RNAi- resistant; cb-unc-119(+)]II	Woodruff et al., 2015
OD1359	unc-119(ed3)III; ltSi716 [pOD1935/pDC208; Pmex-5::EBP-2::GFP::tbb-2; cb-unc-119(+)]I	Wang et al., 2015
OD1959	unc-119(ed9) III; ltSi654 [pVV103; Pspd-2::GFP::SPD-5 reencoded; cb-unc-119(+)]I	Wueseke et al., 2016
OD2879	gsp-2(lt27 [GFP::gsp-2)] unc-119(ed3) III?; ltIs37 [pAA64; pie-1/mCherry::his-58; unc-119 (+)] IV	Hattersley et al., 2016
OD3421	unc-119(ed3)III?; ltIs37 [pAA64; pie-1/mCherry::his-58; unc-119 (+)] IV;gsp-1(lt94 [gfp::gsp-1])V	Kim et al., 2017
EG6699	ttTi5605 II; unc-119(ed3) III; oxEx1578	Frøkjaer-Jensen et al., 2008
EG8081	unc-119(ed3) III; oxTi177 IV.	Frøkjaer-Jensen et al., 2008
ZAN43	ltSi202 [pVV103/pOD1021; Pspd-2::GFP::SPD-5 RNAi-resistant; cb-unc-119(+)]II; ltIs37 [pAA64; pie-1/mCherry::his-58; unc-119 (+)] IV; ltIs28 [pASM14; pie-1/GFP-TEV- Stag::ANI-1; unc-119 (+)];rga-4(ok1935) unc-62(e644) rga-3(ok1988) V/nT1[qIs51] (IV;V)	This study
ZAN57	ltSi654 [pVV103; Pspd-2::GFP::SPD-5 reencoded; cb-unc-119(+)]I; estSi24 [pEZ145; pmex-5::TPXL-1^{WT}::tbb-2; cb-unc-119(+)]II	This study
ZAN59	estSi31 [pEZ150; pmex-5::TPXL-1^{FD}::tbb-2; cb-unc-119(+)]II; unc-119(ed3) III	This study
ZAN103	unc-119(ed3) III; estSi57 [pEZ152; pani-1::mKate2::ANI-1; cb-unc-119(+)]IV	This study
ZAN163	ltSi654 [pVV103; Pspd-2::GFP::SPD-5 reencoded; cb-unc-119(+)]I; estSi31 [pEZ150; pmex-5::TPXL-1^{FD}::tbb-2; cb-unc-119(+)]II	This study
ZAN181	estSi121 [pEZ185; pmex-5::TPXL-1^{WT}::mNeonGreen:: tbb-2; cb-unc-119(+)]II; unc-119(ed3) III	This study
ZAN248	ltSi654 [pVV103; Pspd-2::GFP::SPD-5 reencoded; cb-unc-119(+)]I; estSi31 [pEZ150; pmex-5::TPXL-1^{FD}::tbb-2; cb-unc-119(+)]II; rga-4(ok1935) unc-62(e644) rga-3(ok1988) V/nT1[qIs51](IV;V) estSi57 [pEZ152; pani-1::mKate2::ANI-1; cb-unc-119(+)]IV	This study
ZAN249	ltSi654 [pVV103; Pspd-2::GFP::SPD-5 reencoded; cb-unc-119(+)]I; estSi24 [pEZ145; pmex-5::TPXL-1^{WT}::tbb-2; cb-unc-119(+)]II; rga-4(ok1935) unc-62(e644) rga-3(ok1988) V/nT1[qIs51](IV;V) estSi57 [pEZ152; pani-1::mKate2::ANI-1; cb-unc-119(+)]IV	This study
ZAN267	estSi178 [pEZ231; pmex-5::TPXL-1^{FD}::mNeonGreen:: tbb-2; cb-unc-119(+)]II; unc-119(ed3) III	This study
ZAN286	estSi71 [pAC257;pmex-5::LifeAct::mKate2:tbb2; cb-unc-119(+)]IV; rga-4(ok1935) unc-62(e644) rga-3(ok1988) V/nT1[qIs51](IV;V)	This study

Table S2. **Oligonucleotides used for dsRNA production**

Gene	Oligonucleotide 1 (5′ to 3′)	Oligonucleotide 2 (5′ to 3′)	Template	dsRNA concentration
				mg/ml
tpxl-1	TAATACGACTCACTATAGGACGTCGGTGAGCAAATTGAC	TAATACGACTCACTATAGGTGTACACATATGATGGCACAGG	cDNA	0.58
nmy-2	TAATACGACTCACTATAGGAATTGAATCTCGGTTGAAGGAA	TAATACGACTCACTATAGGACTGCATTTCACGCATCTTATG	cDNA	0.36
hcp-4	TAATACGACTCACTATAGGGGAAATGTACGGAGCGAAAAC	TAATACGACTCACTATAGGGTTGGTGGGTCCAATATTAC	cDNA	0.64
rga-3, rga-4	TAATACGACTCACTATAGGGCAACGCGTCGAAACATCG	TAATACGACTCACTATAGGGTTGGAGTGGCAGTTGGAGTG	Genomic DNA	2.9

T7 sequences are underlined.

References

Frøkjaer-Jensen, C., M.W. Davis, C.E. Hopkins, B.J. Newman, J.M. Thummel, S.-P. Olesen, M. Grunnet, and E.M. Jorgensen. 2008. Single-copy insertion of transgenes in Caenorhabditis elegans. *Nat. Genet.* 40:1375–1383. https://doi.org/10.1038/ng.248

Hattersley, N., D. Cheerambathur, M. Moyle, M. Stefanutti, A. Richardson, K.-Y. Lee, J. Dumont, K. Oegema, and A. Desai. 2016. A nucleoporin docks protein phosphatase 1 to direct meiotic chromosome segregation and nuclear assembly. *Dev. Cell.* 38:463–477. https://doi.org/10.1016/j.devcel.2016.08.006

Kim, T., P. Lara-Gonzalez, B. Prevo, F. Meitinger, D.K. Cheerambathur, K. Oegema, and A. Desai. 2017. Kinetochores accelerate or delay APC/C activation by directing Cdc20 to opposing fates. *Genes Dev.* 31:1089–1094. https://doi.org/10.1101/gad.302067.117

Wang, S., D. Wu, S. Quintin, R.A. Green, D.K. Cheerambathur, S.D. Ochoa, A. Desai, and K. Oegema. 2015. NOCA-1 functions with γ-tubulin and in parallel to Patronin to assemble non-centrosomal microtubule arrays in C. elegans. *eLife*. 4:e08649. https://doi.org/10.7554/eLife.08649

Woodruff, J.B., O. Wueseke, V. Viscardi, J. Mahamid, S.D. Ochoa, J. Bunkenborg, P.O. Widlund, A. Pozniakovsky, E. Zanin, S. Bahmanyar, et al. 2015. Centrosomes. Regulated assembly of a supramolecular centrosome scaffold in vitro. *Science*. 348:808–812. https://doi.org/10.1126/science.aaa3923

Wueseke, O., D. Zwicker, A. Schwager, Y.L. Wong, K. Oegema, F. Jülicher, A.A. Hyman, and J.B. Woodruff. 2016. Polo-like kinase phosphorylation determines Caenorhabditis elegans centrosome size and density by biasing SPD-5 toward an assembly-competent conformation. *Biol. Open*. 5:1431–1440. https://doi.org/10.1242/bio.020990

Zanin, E., A. Desai, I. Poser, Y. Toyoda, C. Andree, C. Moebius, M. Bickle, B. Conradt, A. Piekny, and K. Oegema. 2013. A conserved RhoGAP limits M phase contractility and coordinates with microtubule asters to confine RhoA during cytokinesis. *Dev. Cell.* 26:496–510. https://doi.org/10.1016/j.devcel.2013.08.005